Dentomaxillofacial Radiology (2018) 47, 20170399

birpublications.org/dmfr

RESEARCH ARTICLE

Comparison of the accuracy of periapical radiography with CBCT taken at 3 different voxel sizes in detecting simulated endodontic complications: an ex vivo study

[1]Cemre Koç, [2]Gül Sönmez, [3]Funda Yılmaz, [4]Sevilay Karahan and [5]Kıvanç Kamburoğlu

[1]Endodontics, Başkent University, Faculty of Dentistry, Ankara, , Turkey; [2]Dentomaxillofacial Radiology, Ankara University, Faculty of Dentistry, Ankara, , Turkey; [3]Endodontics, Ankara University, Faculty of Dentistry, Ankara, , Turkey; [4]Biostatistics, Hacettepe University, Faculty of Medicine, Ankara, , Turkey; [5]Dentomaxillofacial Radiology, Ankara University, Faculty of Dentistry, Ankara, , Turkey

Objectives: To compare the accuracy of a photostimulable phosphor plate sensor with cone beam CT (CBCT) images in the detection of simulated endodontic complications.
Methods: Following simulated endodontic complications were created in 40 extracted human mandibular molar teeth: Group 1, Instrument separation (N = 10); Group 2, Strip perforation (N = 10); Group 3, Underfilling of root canals (N = 10); Group 4, Overfilling of root canals (N = 10). Intraoral and CBCT images (voxel size: 0.075, 0.1 and 0.2 mm) were taken. Images were scored by 4 observers according to a 5-point scale. Weighted kappa and intraclass correlation coefficients were calculated. Receiveroperating characteristic analysis was performed and DeLong test was used to compare areaunder curve values. Significance level was set at $p < 0.05$.
Results: Intraobserver kappa ranged from moderate (0.417) to excellent (0.918). Intraclass correlation coefficients ranged from moderate (0.482) to excellent (0.855). For Group 1 (instrument separation) the highest Az values were obtained for intraoral images and the lowest for CBCT (0.2 mm voxel size) ($p < 0.05$). The highest Az values were obtained for Group 2 (strip perforation) among all groups. With all CBCT image settings, observers performed similarly and better than intraoral images ($p < 0.05$) in detection of strip perforation. For Group 3 (underfilling), higher Az values for CBCT images were obtained compared to intraoral images without statistically significant difference ($p > 0.05$). For Group 4 (overfilling), higher Az values for CBCT images were obtained when compared to digital intraoral for observer 1 and 2 ($p < 0.05$).
Conclusions: CBCT images may be useful as an adjunct to periapical imaging in the detection of endodontic complications, such as strip perforation and overfilled root canals.
Dentomaxillofacial Radiology (2018) **47**, 20170399. doi: 10.1259/dmfr.20170399

Cite this article as: Koç C, Sönmez G, Yılmaz F, Karahan S, Kamburoğlu K. Comparison of the accuracy of periapical radiography with CBCT taken at 3 different voxel sizes in detecting simulated endodontic complications: an ex vivo study. *Dentomaxillofac Radiol* 2018; **47**: 20170399.

Keywords: Instrument separation; strip perforation; underfilling; overfilling; CBCT

Introduction

Endodontic complications can be experienced at all stages during root canal therapy and they may increase the risk of failure in the presence of concomitant infection.[1] A common complication is instrument separation and may occur due to existence of complex root canal morphology, improper use and/or overuse of the instrument.[2,3] As a result, in case of instrument separation, removal of residual infected tissue[4] and effective

Correspondence to: Dr Kıvanç Kamburoğlu, E-mail: dtkivo@yahoo.com; kamburogluk@dentistry.ankara.edu.tr
Received 25 October 2017; revised 12 December 2017; accepted 17 January 2018

root canal disinfection[5] may be hindered. The risk of root fracture or root perforation is also increased by the attempts to remove or bypass the separated instrument.[6,7] Another complication is the strip perforation that indicates excessive use of instruments and the thinning of the lateral root wall. It occurs in the coronal third of the root canal or below of the furcation level and has poorer prognosis than perforation that exists in the middle or apical third of the root canal.[8] Electronic apex locators, operative microscopes are useful tools for detecting perforation but they are ineffective in endodontically filled root canals.[9,10] Determining adequate length of root canal filling influences endodontic success[11] since underfillings provide a space for bacterial penetration and overfillings cause sustained irritation to periapical tissues.[12,13] However, controversial issues related to determination of the optimal root canal instrumentation and obturation length due to histologic and anatomic factors still remain unresolved.[14]

Early determination of these complications is essential in terms of both deciding appropriate treatment procedures and preventing medico-legal actions.[15] Periapical radiography provides valuable information for the identification and localization of these complications in the mesiodistal dimensions, however; it lacks information in the buccolingual dimensions. Cone beam CT (CBCT) allows the visualization of teeth and related structures in different planes without superimposition of anatomic structures and geometric distortion and therefore the use of CBCT is suggested for the diagnosis of complex endodontic situations in cases where two-dimensional techniques fail to reveal sufficient information.[16–18] A limitation of the CBCT systems is artifacts that include streaks around materials as well as dark zones which are induced in the presence of high density materials, such as root canal filling or metal post. These artifacts may negatively affect image quality and diagnostic ability of CBCT scans.[19] In CBCT imaging, reconstruction image is acquired by isotropic voxels that can be as small as 0.075 to 0.4 mm. Voxel size is detrimental in terms of diagnostic quality and scanning and reconstruction times of CBCT images.[20]

In view of the importance of difficulties in radiological diagnosis of endodontic complications around high density materials and considering possible differences between intraoral radiography and various types of CBCT images, the objective of the present study was to compare the accuracy of an intraoral phosphor plate sensor with CBCT obtained at 3 different voxel sizes in detecting simulated endodontic complications.

Methods and materials

This study protocol was approved by the ethics committee of Ankara University Dentistry Faculty, Ankara, Turkey (36290600/111). In order to analyze inter-methods and inter-observer compatibility with a maximum error of 10%, it is necessary to include at least 40 teeth for 4 groups each comprising 10 teeth at 75% power and 5% Type 1 error levels. Our study comprised 40 human mandibular molar teeth that were extracted for periodontal or orthodontic reasons.Teeth were selected and stored in distilled water at room temperature. Teeth with external or internal root resorption, anomalies, fracture, crack and immature apices were not included in the study. Endodontic access cavities were prepared and canal patency was checked by using a #10 K-file. A #10 K-file was introduced into the canal until its tip was just visible at the apical foramen and the working length was determined to be 1 mm short from calculated real canal length. In each tooth, two mesial canals were instrumented in a crown down manner with Protaper Next rotary systems (PTN, Dentsply Maillefer, Ballaigues, Switzerland) up to X2 file (size 25, apical taper 6%). During instrumentation procedure, canals were irrigated with 2.5% NaOCl solution at each change of instrument. In 40 teeth, simulated endodontic complications were performed in one of two mesial canals and that root canal was selected randomly (mesiobuccal or mesiolingual) and noted. The other mesial canal without endodontic complication served as control. Teeth (n = 40) were divided into four groups and the following simulated endodontic complications were performed: Group 1, Instrument separation (n = 10); Group 2, Strip perforation (n = 10); Group 3, Underfilling of root canals (n = 10); Group 4, Overfilling of root canals (n = 10). Simulated endodontic complications were created as follows: Group 1, Instrument separation: After root canal instrumentation, a fracture point was created on the 2 mm apical portion of the Protaper X2 file. That file was inserted into the canal and rotated at the end of the canal. Rest of the root canals were filled with AH Plus (Dentsply, DeTrey, Konstanz, Germany) root canal sealer and gutta percha single cones of which 2 mm portions of them were cut. Group 2, Strip perforation: After root canal instrumentation, gates glidden drill no. 2 or no. 3 (Dentsply Maillefer, Ballaigues, Switzerland) was used in the coronal third of root canal until the perforation was created at the distal surface of the mesial canal. The perforation defect was confirmed by a size 20 K-file through root canal. The root canals were then filled with gutta percha single cones and AH Plus (Dentsply, DeTrey, Konstanz, Germany) root canal sealer. Group 3, Underfilling of the root canals: In this group, root canal preparations were performed 2 mm short from the determined working length and root canals were underfilled with gutta-percha single cones and AH Plus (Dentsply, DeTrey, Konstanz, Germany) root canal sealer. Group 4, Overfilling of the root canals: In this group, root canal preparations were performed 2 mm beyond the determined working length during instrumentation and thereby root canals were overfilled with gutta-percha single cones and AH Plus (Dentsply, DeTrey, Konstanz, Germany) root canal sealer.

For imaging procedures, each tooth was randomly placed in the appropriately prepared mandibular molar sockets of a dry mandible covered with 2 cm red wax soft tissue equivalent in groups of 4 (2 molars on left

side and 2 molars on right side) in contact. Each tooth was then randomly placed in the sockets regardless of which endodontic complication was performed in the tooth. Digital intraoral periapical radiographs were exposed with a Gendex X-ray machine (Gendex Digital Systems, Hatfield, PA) operated at 65 kVp and 7 mA and GXPS-500 PSP (photostimulable phosphor plate) (Gendex Digital Systems, Hatfield, PA) detector size 2. Image recording was set at a 64 μm (high) pixel size, 32 bit color and 14.3 lp mm^{-1} spatial resolution. Each tooth was imaged 2 times at two different horizontal planes of the X-ray tube (buccolingual in orthoradial and disto-radial) with a 15° angle after placing the mandible on a specific jig for horizontal angulation. *Ex vivo* imaging was performed using standardized paralleling technique equipment with rectangular collimation (Rinn Manufacturing Company, Elgin, IL) with a focus-receptor distance of 40 cm and an image-exposure time of 0.25 s. Exposure time was determined by consensus. Pulpal root canal, dentine and enamel visibility were used as indicators of optimal image quality. In addition, CBCT images at three different voxel sizes (0.075 , 0.1 and 0.2 mm) were obtained at 96 kVp, 1 mA with a 55 × 50 mm FOV and exposure times ranging between 12 and 15 s by using ProMax® 3D Max CBCT unit (Planmeca, Helsinki, Finland). Finally, a total of 4 image sets were obtained as follows: (1) CBCT 0.075 mm voxel size; (2) CBCT 0.1 mm voxel size; (3) CBCT 0.2 mm voxel size; and (4) PSP.

A specific calibration session by using 10 images which were not included in the study was conducted prior to interpretation process. Image sets were viewed separately by 4 blinded, calibrated and experienced observers in digital intraoral radiography and CBCT assessment (2 dentomaxillofacial radiologists and 2 endodontists) in a dimly lit room. No time restriction was placed on the observers. Image sets were viewed at 1-week intervals, and evaluations of each image set were repeated 1 week after the initial viewings. All images were randomized within each imaging protocol. By using dedicated softwares and reformatted multiplanar sections including axial, coronal, parasagittal and cross-sectional views of the systems and built-in enhancement tools if deemed necessary, observers were asked to diagnose mentioned complications on a 22″ NEC MD213MG LCD monitor (NEC, Tokyo, Japan), at a screen resolution of 2048 × 1536 pixel and 32-bit color depth. The presence or absence of four simulated endodontic complications for each tooth was scored according to a 5-point scale as follows: (1) definitely present; (2) probably present; (3) uncertain/ unable to tell; (4) probably absent; and (5) definitely absent. Figure 1 shows 4 different simulated complications imaged with PSP sensor and CBCT with 3 different voxel sizes.

Statistical analysis

Weighted kappa and intraclass correlation coefficients were calculated to assess the intra- and interobserver agreement for each display type, respectively. Kappa values were interpreted as the following criteria: <0.10 = no agreement; 0.10–0.40 = poor agreement; 0.41–0.60 = moderate agreement; 0.61–0.80 = strong agreement; and 0.81–1.00 = excellent agreement.[21] Scores obtained from different CBCT display types were compared with the gold standard using the receiver operating characteristic analysis to evaluate the observers' ability to differentiate between teeth with and without simulated endodontic complications. The area under the receiver operating characteristic curves (Az) with standard errorE) and 95% confidence interval (CI) were calculated using the SPSS v. 11.5 (SPSS Inc., Chicago, IL). Thus, the Az value 1, corresponds to perfect discrimination, whereas values under 0.5, corresponds to scores with no discrimination ability. Therefore, Az values for each image mode, observer and complication type were compared using *z* tests against Az = 0.5. Significance level was set at $p = 0.05$. Sensitivity (Se), specificity (Sp), positive predictive value (PPV) and negative predictive value (NPV) were also calculated. DeLong test was used to compare area under curve(AUC) values for different image sets and significance level was set at $p < 0.05$.

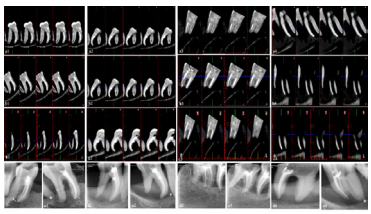

Figure 1 Images taken for the detection of four different endodontic complications as follows: Groups of instrument separation (1), strip perforation (2), underfilling (3), and overfilling (4). (a1–a4) CBCT images were taken at 0.075 mm voxel size. (b1–b4) CBCT images were taken at 0.1 mm voxel size. (c1–c4) CBCT images were taken at 0.2 mm voxel size. (d1–d4) PSP images were taken from distoradial view. (e1–e4) PSP images were taken form orthoradial view. CBCT, cone beam CT; PSP, photostimulable phosphor plate.

Results

For all image sets and groups of complications, the intraobserver kappa values ranged from moderate (0.417) to strong (0.782) for observer 1, from moderate (0.511) to excellent (0.916) for observer 2, from strong (0.710) to excellent (0.918) for observer 3, and from moderate (0.597) to excellent (0.816) for observer 4. Intraclass correlation coefficients ranged from moderate (0.482) to strong (0.778) for the 1st readings and from strong (0.666) to excellent (0.855) for the 2nd readings. We found similar kappa coefficients and intraclass correlation coefficients values considering image sets and groups of complications.

Table 1 shows the AUC (Az) values, sensitivity, specificity, PPV, and NPV calculated for all observers and image sets for Group 1 (instrument separation) for the 1st readings. Calculated AUC values

Table 1 AUCvalues, Se, Sp, PPV and NPV for all observers, image sets and Group 1 (instrument separation)

		AUC values	*SE*[a]	*Asymptotic sig.*[b]	*Asymptotic 95% confidence interval*		*Se*	*Sp*	*PPV*	*NPV*
					Lower bound	*Upper bound*				
Observer 1	CBCT 0.075 mm voxel size	.736	.080	.016	.579	.893	.200	.985	.667	.893
	CBCT 0.1 mm voxel size	.683	.110	.063	.468	.898	.400	.985	.800	.918
	CBCT 0.2 mm voxel size	.568	.101	.492	.370	.765	.200	.912	.250	.886
	Digital intraoral radiography	.871	.062	.000	.750	.992	.800	.794	.381	.964
Observer 2	CBCT 0.075 mm voxel size	.729	.104	.020	.525	.934	.500	.971	.714	.930
	CBCT 0.1 mm voxel size	.707	.105	.035	.502	.913	.400	.971	.667	.917
	CBCT 0.2 mm voxel size	.699	.100	.043	.503	.895	.300	.956	.500	.903
	Digital intraoral radiography	.814	.092	.001	.634	.994	.700	.912	.538	.954
Observer 3	CBCT 0.075 mm voxel size	.871	.077	.000	.720	1.000	.700	.926	.636	.969
	CBCT 0.1 mm voxel size	.738	.104	.016	.534	.941	.400	.985	.800	.918
	CBCT 0.2 mm voxel size	.600	.108	.309	.389	.811	.100	1.000	1.000	.883
	Digital intraoral radiography	.846	.082	.000	.685	1.000	.800	.824	.444	.966
Observer 4	CBCT 0.075 mm voxel size	.900	.076	.000	.751	1.000	.800	1.000	1.000	.971
	CBCT 0.1 mm voxel size	.898	.076	.000	.748	1.000	.800	.985	.889	.971
	CBCT 0.2 mm voxel size	.829	.093	.001	.647	1.000	.700	.971	.778	.957
	Digital intraoral radiography	.844	.079	.000	.690	.998	.800	.868	.500	.967

AUC, area under curve; CBCT, cone beam CT; NPV, negative predictive value; PPV, positive predictive value; Se, sensitivity; SE, standard error; Sp, specificity.
[a]Statistical error.
[b]Statistical error.

ranged between 0.729 and 0.900 for the CBCT (0.075 mm mm) images, between 0.683 and 0.898 for the CBCT (0.1 mm voxel size) images, between 0.568 and 0.829 for the CBCT (0.2 mm voxel size) images, and between 0.814 and 0.871 for the digital intraoral images. In general, the highest Az and sensitivity values were obtained for image set 4 (digital intraoral images) and the lowest for image set 3 (CBCT with 0.2 mm voxel size). We found statistically significantly higher Az values for image set 4 (digital intraoral images) when compared to image set 3 (CBCT with 0.2 mm voxel size) for observer 1 ($p < 0.001$). In addition, for observer 3, Az values found for image set 3 (CBCT with 0.2 mm voxel size) were statistically significantly lower than those of image set 1 ($p = 0.001$) and 4 ($p = 0.004$). However, comparison of Az values for CBCT images at all voxel sizes and digital periapical images showed no statistically significant differences between image sets for observer 2 and obsever 4.

Table 2 shows the AUC (Az) values, sensitivity, specificity, PPV, and NPV calculated for all observers and image sets for Group 2 (strip perforation) for the 1st readings. In general, the highest Az, Se, Sp, PPV and NPV values were obtained for Group 2 (strip perforation) when compared to the other groups. Calculated AUC values ranged between 0.915 and 0.993 for the CBCT (0.075 mm voxel size) images, between 0.941 and 0.999 for the CBCT (0.1 mm voxel size) images, between 0.884 and 0.998 for the CBCT (0.2 mm voxel size) images, and between 0.522 and 0.676 for the digital intraoral images. For observers 1, 3 and 4 CBCT images obtained at all voxel sizes (image sets 1, 2 and 3) performed similarly and better than intraoral images (image set 4) for the detection of strip perforation (Observer 1: $p = 0.019$, 0.001 and 0.01; Observer 3: $p < 0.0001$; Observer 4: $p = 0.0002$, 0.0001 and 0.0001, for image sets 1, 2 and 3, respectively). Statistically significant differences ($p < 0.05$) were found between the Az values of all CBCT image sets and intraoral images. For observer 2, Az values calculated for image sets 1, 2 and 3 were found to be statistically significantly higher than those of image set 4 ($p = 0.001$, $p = 0.001$ and $p = 0.003$, respectively). In addition, with image sets 1 and 2, observer 2 performed similarly and better when compared to image set 3 ($p = 0.047$ and $p = 0.013$, respectively).

Table 3 shows the AUC (Az) values, sensitivity, specificity, PPV, and NPV calculated for all observers and image sets for Group 3 (underfilling) for the 1st readings. In general, higher Az values for CBCT images were obtained when compared to digital intraoral images without statistically significant difference ($p > 0.05$). Calculated AUC values ranged between 0.518 and 0.774 for the CBCT (**0.075** mm voxel size) images, between 0.592 and 0.779 for the CBCT (0.1 mm voxel size) images, between 0.613 and 0.748 for the CBCT (0.2 mm voxel size) images, and between 0.480 and 0.716 for the digital intraoral images. No statistically significant differences were found among different image sets for the detection of underfilled root canals ($p > 0.05$).

Table 4 shows the AUC (Az) values, sensitivity, specificity, PPV, and NPV calculated for all observers and image sets for Group 4 (overfilling) for the 1st

Table 2 AUCvalues, Se, Sp, PPV and NPV for all observers, image sets and Group 2 (strip perforation)

		AUC values	*SE*[a]	*Asymptotic sig.*[b]	*Asymptotic 95% confidence interval*		*Se*	*Sp*	*PPV*	*NPV*
					Lower bound	*Upper bound*				
Observer 1	CBCT 0.075 mm voxel size	.915	.075	.000	.768	1.000	.900	.897	.643	.984
	CBCT 0.1 mm voxel size	.979	.015	.000	.951	1.000	1.000	.956	.769	1.000
	CBCT 0.2 mm voxel size	.990	.010	.000	.970	1.000	.900	.853	.900	1.000
	Digital intraoral radiography	.615	.098	.241	.423	.808	.200	.897	.500	.884
Observer 2	CBCT 0.075 mm voxel size	.932	.059	.000	.817	1.000	.800	.985	.889	.971
	CBCT 0.1 mm voxel size	.941	.058	.000	.827	1.000	.800	1.000	1.000	.971
	CBCT 0.2 mm voxel size	.884	.066	.000	.755	1.000	.500	1.000	1.000	.932
	Digital intraoral radiography	.631	.105	.183	.424	.837	.300	.912	.375	.899
Observer 3	CBCT 0.075 mm voxel size	.993	.009	.000	.975	1.000	1.000	.985	.909	1.000
	CBCT **0.1** mm voxel size	.992	.009	.000	.974	1.000	1.000	.985	.909	1.000
	CBCT **0.2** mm voxel size	.990	.010	.000	.970	1.000	.800	.985	.889	.971
	Digital intraoral radiography	.522	.101	.823	.323	.721	.100	.971	.333	.880
Observer 4	CBCT 0.075 mm voxel size	.993	.009	.000	.975	1.000	1.000	.971	.833	1.000
	CBCT 0.1 mm voxel size	.999	.002	.000	.994	1.000	.900	.985	.900	.985
	CBCT 0.2 mm voxel size	.998	.003	.000	.991	1.000	.900	1.000	1.000	.986
	Digital intraoral radiography	.676	.107	.073	.467	.886	.400	.941	.667	.914

AUC, area under curve; CBCT, cone beam CT; NPV, negative predictive value; PPV, positive predictive value; Se, sensitivity; SE, standard error; Sp, specificity.
[a]Statistical error.
[b]Statistical error.

readings. Calculated AUC values ranged between 0.772 and 0.921 for the CBCT (0.075 mm voxel size) images, between 0.827 and 0.918 for the CBCT (0.1 mm voxel size) images, between 0.567 and 0.874 for the CBCT (0.2 mm voxel size) images, and between 0.485 and 0.955 for the digital intraoral images. In general,

Table 3 AUCvalues, Se, Sp, PPV and NPV for all observers, image sets and Group 3 (underfilling)

		AUCvalues	*SE*[a]	*Asymptotic sig.*[b]	*Asymptotic 95% confidence interval*		*Se*	*Sp*	*PPV*	*NPV*
					Lower bound	*Upper bound*				
Observer 1	CBCT 0.075 mm voxel size	.518	.102	.852	.318	.717	.182	.866	.182	.866
	CBCT 0.1 mm voxel size	.592	.101	.329	.394	.790	.273	.896	.300	.882
	CBCT 0.2 mm voxel size	.613	.094	.231	.429	.798	.364	.791	.286	.883
	Digital intraoral radiography	.480	.102	.835	.281	.680	.364	.627	.143	.857
Observer 2	CBCT 0.075 mm voxel size	.685	.095	.050	.498	.872	.545	.746	.261	.909
	CBCT 0.1 mm voxel size	.776	.070	.003	.639	.913	.636	.776	.333	.929
	CBCT 0.2 mm voxel size	.702	.071	.032	.562	.842	.545	.716	.240	.906
	Digital intraoral radiography	.716	.091	.022	.537	.896	.636	.597	.206	.909
Observer 3	CBCT 0.075 mm voxel size	.774	.093	.004	.592	.956	.636	.925	.583	.939
	CBCT 0.1 mm voxel size	.779	.092	.003	.599	.959	.636	.940	.636	.940
	CBCT 0.2 mm voxel size	.748	.093	.009	.567	.930	.364	.896	.400	.923
	Digital intraoral radiography	.683	.099	.053	.489	.878	.364	.896	.400	.909
Observer 4	CBCT 0.075 mm voxel size	.659	.102	.092	.459	.859	.364	.955	.571	.901
	CBCT 0.1 mm voxel size	.657	.102	.096	.458	.857	.364	.955	.571	.901
	CBCT 0.2 mm voxel size	.686	.102	.049	.486	.886	.455	.940	.556	.913
	Digital intraoral radiography	.612	.105	.236	.407	.817	.364	.851	.333	.891

AUC, area under curve; CBCT, cone beam CT; NPV, negative predictive value; PPV, positive predictive value; Se, sensitivity; SE, standard error; Sp, specificity.
[a]Statistical error.
[b]Statistical error.

Table 4 AUCvalues, Se, Sp, PPV and NPV for all observers, image sets and Group 3 (overfilling)

		AUC values	*SE*[a]	*Asymptotic sig.*[b]	*Asymptotic 95% confidence interval*		*Se*	*Sp*	*PPV*	*NPV*
					Lower bound	*Upper bound*				
Observer 1	CBCT 0.075 mm voxel size	.772	.091	.006	.594	.950	.600	.882	.429	.938
	CBCT 0.1 mm voxel size	.827	.085	.001	.660	.994	.700	.941	.636	.955
	CBCT 0.2 mm voxel size	.567	.099	.496	.374	.760	.100	.897	.200	.884
	Digital intraoral radiography	.485	.111	.881	.268	.702	.400	.559	.129	.884
Observer 2	CBCT 0.075 mm voxel size	.921	.041	.000	.839	1.000	.900	.853	.474	.983
	CBCT 0.1 mm voxel size	.901	.072	.000	.760	1.000	.900	.882	.529	.984
	CBCT 0.2 mm voxel size	.826	.083	.001	.663	.989	.700	.926	.583	.955
	Digital intraoral radiography	.551	.107	.606	.341	.761	.300	.809	.188	.887
Observer 3	CBCT 0.075 mm voxel size	.902	.064	.000	.777	1.000	.900	.779	.375	.981
	CBCT 0.1 mm voxel size	.895	.063	.000	.772	1.000	.900	.809	.409	.982
	CBCT 0.2 mm voxel size	.818	.081	.001	.660	.977	.700	.868	.438	.967
	Digital intraoral radiography	.955	.024	.000	.909	1.000	.900	.897	.643	.984
Observer 4	CBCT 0.075 mm voxel size	.907	.059	.000	.791	1.000	.900	.897	.563	.984
	CBCT 0.1 mm voxel size	.918	.059	.000	.802	1.000	.900	.882	.529	.984
	CBCT 0.2 mm voxel size	.874	.062	.000	.751	.996	.800	.868	.471	.967
	Digital intraoral radiography	.772	.098	.006	.579	.965	.600	.926	.667	.940

AUC, area under curve; CBCT, cone beam CT; NPV, negative predictive value; PPV, positive predictive value; Se, sensitivity; SE, standard error; Sp, specificity.
[a]Statistical error.
[b]Statistical error.

higher Az values for CBCT images were obtained when compared to digital intraoral images. However, only for observer 1 and 2, statistically significant differences were found among image sets. For observer 1, image sets 1 (CBCT with 0.075 mm voxel size) and 2 (CBCT with 0.1 mm voxel size) were found to be better than image set 3 ($p = 0.0294$ and $p = 0.0001$, repectively). In addition, with image set 2 (CBCT with 0.1 mm voxel size), observer 2 performed better when compared to image set 4 (digital intraoral images) ($p = 0.008$).

Discussion

Selection of appropriate imaging parameters for the accurate diagnosis of endodontic complications is important in terms of both decision making and treatment planning. In the present study, all observers assessed CBCT images taken in 3 different voxel sizes using small fixed field-of-view (FOV) (55 × 50 mm) in comparison to periapical imaging. In general, except for the instrument separation group, AUC values for CBCT images were higher than those of periapical images. CBCT images with different voxel sizes performed better when compared to digital intraoral radiographs in detection of strip perforation and performed similarly in detection of underfilled root canals. Digital intraoral images performed better than CBCT images in the detection of instrument separation. The ability of observers by using all image sets was found to be acceptable in identifying simulated endodontic complications depending on the complication type. AUC values revealed that strip perforation was more clearly detected by all observers when compared with the other complications.

We used mandibular molar teeth since they are relatively prone to occurrence of iatrogenic errors during root canal preparation and obturation.[22] Using intraoral radiographic techniques for the detection of simulated endodontic complications in mandibular molars is complicated by superimposition of mesio-buccal or lingual root canals and projection geometry. We assessed periapical images exposed from two angulations in order to provide information from different horizontal views and simulate real clinical practice. Additionally, related endodontic complications were not performed in a specific region (buccal or lingual canal). This situation made it difficult for observers to determine whether there was any complication and if any, in which root canal, endodontic complication was performed. While CBCT imaging allows three dimensional visualization of related region, it is likely that the presence of metallic artifacts from metal posts and root-canal filling materials reduces its diagnostic efficacy.[19] In the present study, observers evaluated simulated endodontic complications in root filled teeth, therefore; observer performance might be negatively influenced by beam hardening artifacts.

To the best of our knowledge, although several previous studies were conducted in order to assess each

endodontic complication separately this study was the first to evaluate simulated complications simultaneously in a random setting, such as instrument separation, strip perforation, underfilled and overfilled root canals.[14,17,23,24] Instrument separation is a common complication which may occur during root canal preparation. It may negatively affect the prognosis of treatment and cause medico-legal actions if not detected early.[25] Our results revealed that digital intraoral images were found to be more effective than CBCT images in detection of instrument separation. Ramos Brito et al,[23] compared CBCT images with different voxel sizes (0.085 and 0.2 mm) to periapical radiographs obtained from three digital systems for detecting fractured instruments with or without root canal filling. Significantly lower sensitivity and accuracy values were obtained from CBCT images in case of the presence of root canal fillings. Similar to our results, no differences were found among CBCT images obtained at different voxel sizes. They acquired digital radiographs with 2 semidirect systems using PSP and 1 direct system using a complementary metal oxide semiconductor (CMOS). Especially, in the presence of root canal filling, CMOS digital system was suggested considering its higher spatial resolution (26.3 lp mm^{-1}) compared to two PSP systems (25 and 14.3 lp mm^{-1}). In the present study, we found higher AUC values for periapical images when compared to CBCT images. This finding may be attributable to observer performance and experience, PSP system [14.3 lp mm^{-1} and 64 μm (high) pixel size], CBCT unit and study design. Another study,[24] found that periapical radiography was superior to CBCT imaging in the detection of separated instruments in root-filled canals in single rooted teeth, regardless of the instrument type or the sealer type. On the other hand, in the absence of root canal filling, CBCT imaging and periapical radiographs presented similar accuracy in detection of fractured instrument. Metallic artifacts affected the ability to distinguish root canal filling from separated instrument adversely. Unlike the mentioned study, we used mandibular molar teeth, and artifacts created by root canal filling materials may be a reason for the lower AUC values obtained from CBCT images.

Strip perforation occurs during root canal instrumentation. Early detection and repair of perforation site is important for promising prognosis.[26] Our results revealed higher AUC values obtained from all CBCT image sets when compared to periapical images in the detection of strip perforation with statistical significance. Regardless of imaging modalities, all of our observers showed better performance for detecting strip perforationin comparison with others. It is possible that penetration of root canal sealer into perforation site enabled better visualization of this complication. According to a previous study, CBCT imaging provided higher accuracy than periapical radiographs in detection of both strip and root perforations.[17] The concavity of the root was suggested as the reason for inability of periapical radiographs in detection of strip perforations.[17] Also, CBCT-induced artifacts were interpreted as perforations and reduced accuracy of image sets.[17] In the present study, for all observers, the AUC values obtained from CBCT images were found to be statistically significantly higher than periapical radiography in detection of strip perforation. In addition, generally, no statistically significant difference was found among various CBCT voxel sizes. A previous study[27] compared CBCT images with different voxel sizes (0.1, 0.15, 0.2, and 0.4 mm) to an intraoral sensor in the detection of furcation perforations. All CBCT images taken at different voxel sizes performed similarly. Besides, CBCT images at all voxel sizes performed better than intraoral PSP sensor. In the mentioned study,[27] teeth without root canal filling were included; therefore, influence of beam hardening artifacts on observer performance was not an issue. Obviously, artificially preprared perforations in *ex vivo* studies may not be able to reflect the actual clinical conditions.

Accurate determination of root canal obturation length is still questionable.[14] However, it was suggested that root canal instrumentation and obturation should not extend beyond apex.[28,29] According to a meta-analysis[30] which assessed different obturation lengths with regard to endodontic success and failure the best prognosis for endodontic treatment was associated with obturation 0 to 1.0 mm short from the apex. In addition, the success rates were higher for obturation beyond the radiographic apex (28.9%) compared to obturation 1.0 to 3.0 mm short from the apex (5.9%). Therefore, in this present study, we conducted root canal instrumentation and obturation that extend 2 mm beyond or 2 mm short of the determined working length in overfilling and underfilling groups, respectively. Another study,[31] compared *in vivo* performance characteristics of CBCT and periapical radiography in the evaluation of root canal obturation and included 323 roots that required endodontic microsurgery and had periapical radiographs and CBCT images taken before. For assessing the apical extension of root canal obturations, CBCT was found to be better than periapical radiography. However, both techniques underestimated the overextensions of root canal obturations. Cheng et al,[14]analyzed root canals that were obturated 0–2 mm short of the radiographic apex by using periapical radiography and CBCT. CBCT diagnosed 30.3% of root canal obturations with radiographically adequate length as "inadequate". Also, 13.8% of teeth was classified as overextension and 16.5% of teeth was classified as underextension. In accordance with these results, we generally obtained higher AUC values from CBCT images when compared to periapical images for detecting overfilled root canals with statistically significant differences for two observers. However, in our study, no image sets showed superiority to each other for detection of underfilled root canals. This can be due to misinterpretation of CBCT images in assessing root canal obturation lengths. Decurcio et al,[32] reported

that dimensions of root canal fillings were greater on CBCT images than on the original root specimens as a result of artifacts. Aforementioned drawbacks of CBCT imaging and periapical radiography constitute a limitation for the detection of underfilled and overfilled root canals. Studies are being conducted to overcome the unfavorable effects of artifacts on interpreting CBCT images. A previous study,[33] that evaluated the influence of CBCT filters on diagnosis of simulated endodontic complications such as fractured file, perforations in the canal walls, deviated cast post, and external root resorption, reported that the filters did not improve the diagnosis of the endodontic complications. Specifically, diagnosis of fractured file and perforation in the canal walls were found to be difficult tasks. Another study,[34] reported that all CBCT images exposed without and with different artifact reduction modes performed similarly in diagnosis of simulated furcal perforations in root filled teeth. Eskandarloo et al[16] found better sensitivity and specificity values for detecting various complications with the CBCT unit utilized in the present study when compared to NewTom CBCT unit. Additionally, the authors reported that creating artifacts could vary among different CBCT machines. Technical specifications of the CBCT unit, software capabilities, settings and display options along with the observer performance may all affect the sensitivity and specificity values for a specific diagnostic purpose.

In the present study, we also investigated the influence of different voxel sizes on observer ability to detect simulated complications by using the smallest FOV available. CBCT still delivers far greater effective doses when compared to intraoral imaging. The effective dose for the CBCT unit utilized in the present study is in the range 28 to 122 μSv.[35] This is higher than the effective doses from periapical radiography taken with PSP with rectangular collimation (0.1 to 2.6 μSv).[36] Therefore, clinicians should use caution when prescribing CBCT imaging for the detection of endodontic complications. Besides, voxel size is one of the most important CBCT parameters that affected image quality, and it is related to scanning and reconstruction times of CBCT images. Thus, determination of optimal CBCT parameters is crucial in terms of radiation exposure and safety. In general, we found no statistically significant difference among CBCT images taken with the three different voxel sizes, and therefore; considering the increase in radiation dose and noise when using smaller voxel sizes with limited small FOV, CBCT images taken between 0.1 and 0.2 mm voxel sizes may be suitable in the detection of endodontic complications when necessary.

Conclusion

Given the limitations of the present *ex vivo* research, in general except for the instrument separation group, we found that CBCT images taken with different voxel sizes revealed higher AUC values when compared to intraoral periapical images. CBCT images with different voxel sizes performed better when compared to digital intraoral radiographs in the detection of strip perforation and performed similarly in the detection of underfilled root canals. Although, CBCT is not suggested as a routine imaging modality, it may be utilized as a supplementary method in the detection of endodontic complications when periapical imaging is found to be insufficient. CBCT images obtained between 0.1 and 0.2 mm voxel sizes would be useful in the detection of endodontic complications. Further studies are essential to overcome the limitations of common imaging modalities.

References

1. Lin LM, Rosenberg PA, Lin J. Do procedural errors cause endodontic treatment failure? *J Am Dent Assoc* 2005; **136**: 187–93. doi: https://doi.org/10.14219/jada.archive.2005.0140
2. Shen Y, Coil JM, McLean AG, Hemerling DL, Haapasalo M. Defects in nickel-titanium instruments after clinical use. Part 5: single use from endodontic specialty practices. *J Endod* 2009; **35**: 1363–7. doi: https://doi.org/10.1016/j.joen.2009.07.004
3. Sattapan B, Nervo GJ, Palamara JE, Messer HH. Defects in rotary nickel-titanium files after clinical use. *J Endod* 2000; **26**: 161–5. doi: https://doi.org/10.1097/00004770-200003000-00008
4. Saunders JL, Eleazer PD, Zhang P, Michalek S. Effect of a separated instrument on bacterial penetration of obturated root canals. *J Endod* 2004; **30**: 177–9. doi: https://doi.org/10.1097/00004770-200403000-00012
5. Di Fiore PM, Genov KA, Komaroff E, Li Y, Lin L. Nickel-titanium rotary instrument fracture: a clinical practice assessment. *Int Endod J* 2006; **39**: 700–8. doi: https://doi.org/10.1111/j.1365-2591.2006.01137.x
6. Fu M, Zhang Z, Hou B. Removal of broken files from root canals by using ultrasonic techniques combined with dental microscope: a retrospective analysis of treatment outcome. *J Endod* 2011; **37**: 619–22. doi: https://doi.org/10.1016/j.joen.2011.02.016
7. Madarati AA, Qualtrough AJ, Watts DC. Effect of retained fractured instruments on tooth resistance to vertical fracture with or without attempt at removal. *Int Endod J* 2010; **43**: 1047–53. doi: https://doi.org/10.1111/j.1365-2591.2010.01783.x
8. Nicholls E. Treatment of traumatic perforations of the pulp cavity. *Oral Surg Oral Med Oral Pathol* 1962; **15**: 603–12. doi: https://doi.org/10.1016/0030-4220(62)90180-9
9. Fuss Z, Assooline LS, Kaufman AY. Determination of location of root perforations by electronic apex locators. *Oral Surg Oral Med Oral Pathol Oral Radiol Endod* 1996; **82**: 324–9. doi: https://doi.org/10.1016/S1079-2104(96)80361-1
10. Kim S, Kratchman S. Modern endodontic surgery concepts and practice: a review. *J Endod* 2006; **32**: 601–23. doi: https://doi.org/10.1016/j.joen.2005.12.010
11. de Chevigny C, Dao TT, Basrani BR, Marquis V, Farzaneh M, Abitbol S, et al. Treatment outcome in endodontics: the Toronto study-phases 3 and 4: orthograde retreatment. *J Endod* 2008; **34**: 131–7. doi: https://doi.org/10.1016/j.joen.2007.11.003
12. van der Sluis LW, Wu MK, Wesselink PR. An evaluation of the quality of root fillings in mandibular incisors and maxillary and mandibular canines using different methodologies. *J Dent* 2005; **33**: 683–8. doi: https://doi.org/10.1016/j.jdent.2005.01.007

13. Ricucci D, Langeland K. Apical limit of root canal instrumentation and obturation, part 2. A histological study. *Int Endod J* 1998; **31**: 394–409. doi: https://doi.org/10.1046/j.1365-2591.1998.00183.x
14. Cheng L, Zhang R, Yu X, Tian Y, Wang H, Zheng G, et al. A comparative analysis of periapical radiography and cone-beam computerized tomography for the evaluation of endodontic obturation length. *Oral Surg Oral Med Oral Pathol Oral Radiol Endod* 2011; **112**: 383–9. doi: https://doi.org/10.1016/j.tripleo.2011.04.025
15. Givol N, Rosen E, Taicher S, Tsesis I. Risk management in endodontics. *J Endod* 2010; **36**: 982–4. doi: https://doi.org/10.1016/j.joen.2010.03.030
16. Eskandarloo A, Mirshekari A, Poorolajal J, Mohammadi Z, Shokri A. Comparison of cone-beam computed tomography with intraoral photostimulable phosphor imaging plate for diagnosis of endodontic complications: a simulation study. *Oral Surg Oral Med Oral Pathol Oral Radiol* 2012; **114**: e54–e61. doi: https://doi.org/10.1016/j.oooo.2012.05.026
17. Shemesh H, Cristescu RC, Wesselink PR, Wu MK. The use of cone-beam computed tomography and digital periapical radiographs to diagnose root perforations. *J Endod* 2011; **37**: 513–6. doi: https://doi.org/10.1016/j.joen.2010.12.003
18. D'Addazio PS, Campos CN, Özcan M, Teixeira HG, Passoni RM, Carvalho AC. A comparative study between cone-beam computed tomography and periapical radiographs in the diagnosis of simulated endodontic complications. *Int Endod J* 2011; **44**: 218–24. doi: https://doi.org/10.1111/j.1365-2591.2010.01802.x
19. Vasconcelos KF, Nicolielo LF, Nascimento MC, Haiter-Neto F, Bóscolo FN, Van Dessel J, et al. Artefact expression associated with several cone-beam computed tomographic machines when imaging root filled teeth. *Int Endod J* 2015; **48**: 994–1000. doi: https://doi.org/10.1111/iej.12395
20. Spin-Neto R, Gotfredsen E, Wenzel A. Impact of voxel size variation on CBCT-based diagnostic outcome in dentistry: a systematic review. *J Digit Imaging* 2013; **26**: 813–20. doi: https://doi.org/10.1007/s10278-012-9562-7
21. Landis JR, Koch GG. The measurement of observer agreement for categorical data. *Biometrics* 1977; **33**: 159–74. doi: https://doi.org/10.2307/2529310
22. Yousuf W, Khan M, Mehdi H. Endodontic procedural errors: frequency, type of error, and the most frequently treated tooth. *Int J Dent* 2015; **2015**: 1–7. doi: https://doi.org/10.1155/2015/673914
23. Ramos Brito AC, Verner FS, Junqueira RB, Yamasaki MC, Queiroz PM, Freitas DQ, et al. Detection of fractured endodontic instruments in root canals: comparison between different digital radiography systems and cone-beam computed tomography. *J Endod* 2017; **43**: 544–9. doi: https://doi.org/10.1016/j.joen.2016.11.017
24. Rosen E, Venezia NB, Azizi H, Kamburoğlu K, Meirowitz A, Ziv-Baran T, et al. A comparison of cone-beam computed tomography with periapical radiography in the detection of separated instruments retained in the apical third of root canal-filled teeth. *J Endod* 2016; **42**: 1035–9. doi: https://doi.org/10.1016/j.joen.2016.04.016
25. Panitvisai P, Parunnit P, Sathorn C, Messer HH. Impact of a retained instrument on treatment outcome: a systematic review and meta-analysis. *J Endod* 2010; **36**: 775–80. doi: https://doi.org/10.1016/j.joen.2009.12.029
26. Tsesis I, Fuss ZVI. Diagnosis and treatment of accidental root perforations. *Endod Topics* 2006; **13**: 95–107. doi: https://doi.org/10.1111/j.1601-1546.2006.00213.x
27. Kamburoğlu K, Yeta EN, Yılmaz F. An ex vivo comparison of diagnostic accuracy of cone-beam computed tomography and periapical radiography in the detection of furcal perforations. *J Endod* 2015; **41**: 696–702. doi: https://doi.org/10.1016/j.joen.2014.12.014
28. Moura MS, Guedes OA, De Alencar AH, Azevedo BC, Estrela C. Influence of length of root canal obturation on apical periodontitis detected by periapical radiography and cone beam computed tomography. *J Endod* 2009; **35**: 805–9. doi: https://doi.org/10.1016/j.joen.2009.03.013
29. Wu MK, Wesselink PR, Walton RE. Apical terminus location of root canal treatment procedures. *Oral Surg Oral Med Oral Pathol Oral Radiol Endod* 2000; **89**: 99–103.
30. Schaeffer MA, White RR, Walton RE. Determining the optimal obturation length: a meta-analysis of literature. *J Endod* 2005; **31**: 271–4. doi: https://doi.org/10.1097/01.don.0000140585.52178.78
31. Song D, Zhang L, Zhou W, Zheng Q, Duan X, Zhou X, et al. Comparing cone-beam computed tomography with periapical radiography for assessing root canal obturation in vivo using microsurgical findings as validation. *Dentomaxillofac Radiol* 2017; **46**: 20160463. doi: https://doi.org/10.1259/dmfr.20160463
32. Decurcio DA, Bueno MR, de Alencar AH, Porto OC, Azevedo BC, Estrela C. Effect of root canal filling materials on dimensions of cone-beam computed tomography images. *J Appl Oral Sci* 2012; **20**: 260–7. doi: https://doi.org/10.1590/S1678-77572012000200023
33. Verner FS, D'Addazio PS, Campos CN, Devito KL, Almeida SM, Junqueira RB. Influence of cone-beam computed tomography filters on diagnosis of simulated endodontic complications. *Int Endod J* 2017; **50**: 1089–96. doi: https://doi.org/10.1111/iej.12732
34. Kamburoğlu K, Yılmaz F, Yeta EN, Özen D. Assessment of furcal perforations in the vicinity of different root canal sealers using a cone beam computed tomography system with and without the application of artifact reduction mode: an ex vivo investigation on extracted human teeth. *Oral Surg Oral Med Oral Pathol Oral Radiol* 2016; **121**: 657–65. doi: https://doi.org/10.1016/j.oooo.2016.01.010
35. Pauwels R, Beinsberger J, Collaert B, Theodorakou C, Rogers J, Walker A, et al. Effective dose range for dental cone beam computed tomography scanners. *Eur J Radiol* 2012; **81**: 267–71. doi: https://doi.org/10.1016/j.ejrad.2010.11.028
36. Granlund C, Thilander-Klang A, Ylhan B, Lofthag-Hansen S, Ekestubbe A. Absorbed organ and effective doses from digital intra-oral and panoramic radiography applying the ICRP 103 recommendations for effective dose estimations. *Br J Radiol* 2016; **89**: 20151052. doi: https://doi.org/10.1259/bjr.20151052